Velocity measurements on Engabreen, Norway

Miriam JACKSON,[1] Ian A. BROWN,[2] Hallgeir ELVEHØY[1]

[1]*Norwegian Water Resources and Energy Directorate (NVE), PO Box 5091 Majorstua, NO-0301 Oslo, Norway*
E-mail: mja@nve.no.
[2]*Department of Physical Geography and Quaternary Geology, Stockholm University, SE-106 91 Stockholm, Sweden*

ABSTRACT. Horizontal velocity measurements on the lower part of Engabreen, Norway, were made from repeat aerial photography. IMCORR software, which has been widely used to measure velocities from satellite images, was used to make the measurements. This is the first known successful use of IMCORR on aerial photographs. Supplementary horizontal velocity measurements were made from repeat measurements of stakes, giving velocities over different periods and also in areas that are too slow-moving to register a measurable velocity after only a few days.

INTRODUCTION

Several different techniques are used to study horizontal velocity on glaciers. Possibly the most common of these has traditionally been performed by setting out stakes on a glacier and measuring the initial position and then subsequent position after a suitable interval. This method is simple but has several disadvantages, including the time taken to set out the stakes and measure them, especially on a relatively large glacier where the stakes may be several kilometres apart. Repeat aerial photography can be used instead of, or to supplement, this technique. The use of multiple images taken at different times of the same part of the glacier makes it possible to obtain a much denser velocity measurement network from little or no fieldwork on the glacier. Both techniques have been used on Engabreen, northern Norway, the two methods providing complementary information on the surface velocity of the glacier.

Engabreen

Engabreen is a 38 km^2 outlet glacier of the Svartisen glacier, northern Norway (Fig. 1). It has a maximum elevation of 1575 m a.s.l., and its terminus is just above sea level at the proglacial lake Engabrevatnet, at 7 m a.s.l. Mass-balance measurements have been performed on Engabreen since 1970 (e.g. Kjøllmoen and others, 2003). Measurements for mass balance have been performed at stakes distributed over the glacier. The mass-balance stakes, as well as some additional stakes, were used in the velocity measurements.

DISPLACEMENT MEASUREMENTS

Measurements of horizontal velocity were performed on Engabreen using repeat aerial photography on the lower part and using repeat measurements of stakes distributed over the remainder of the glacier. The photogrammetric measurements are described first.

Repeat aerial photography

Repeat aerial photography has been used extensively to measure velocity on glaciers (e.g. Brecher, 1986; Krimmel, 2001). The technique was subsequently applied to optical satellite imagery (Scambos and Bindschadler, 1993) and synthetic aperture radar images (Lucchitta and Rosanova, 1998). In all cases, the technique requires identifiable features in the input images to measure their displacement. The minimum velocity is therefore a function of the temporal separation, co-registration accuracy and image resolution. Hence, much of the application has focused on fast ice streams where displacements are generally on the order of many pixels when using high-resolution satellite images (with resolutions on the order of 10–30 m). At these scales, large crevasses have been typically used, although in aerial photography smaller features such as surface ponds, large moulins and debris may also be identified.

Engabreen was photographed twice, on 20 August and 10 September 2002 (Fig. 2), at a scale of 1 : 15 000, and photography was performed under contract by Fjellanger Widerøe AS, Oslo. The photography was performed at approximately the same time on each day (1144 and 1242 UTC respectively), although the northerly latitude of the glacier and northern orientation of the glacier tongue means that there was much more shadow on the second set of photos, complicating the position measurement of crevasses and other features. The area of the glacier that is suitable for study using repeat aerial photography is the lowermost part that lies below about 940 m a.s.l. and has an area of 4 km^2.

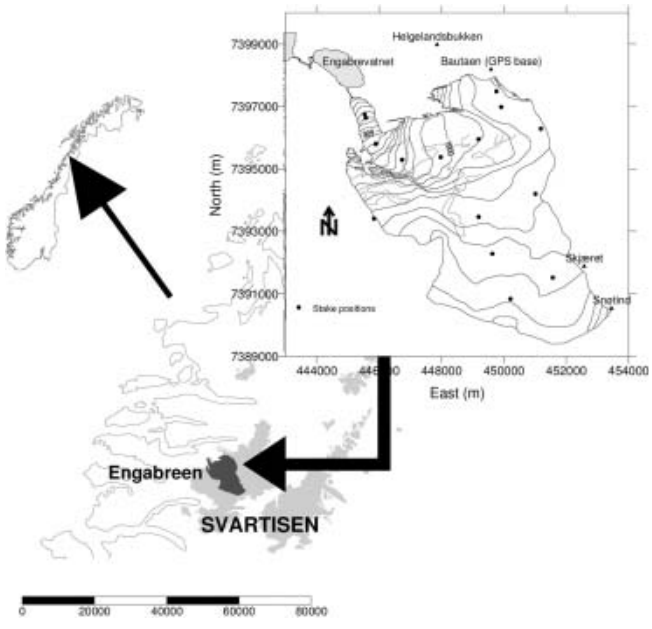


Fig. 1. Location map of Engabreen and Svartisen.

https://doi.org/10.3189/172756405781812655 Published online by Cambridge University Press

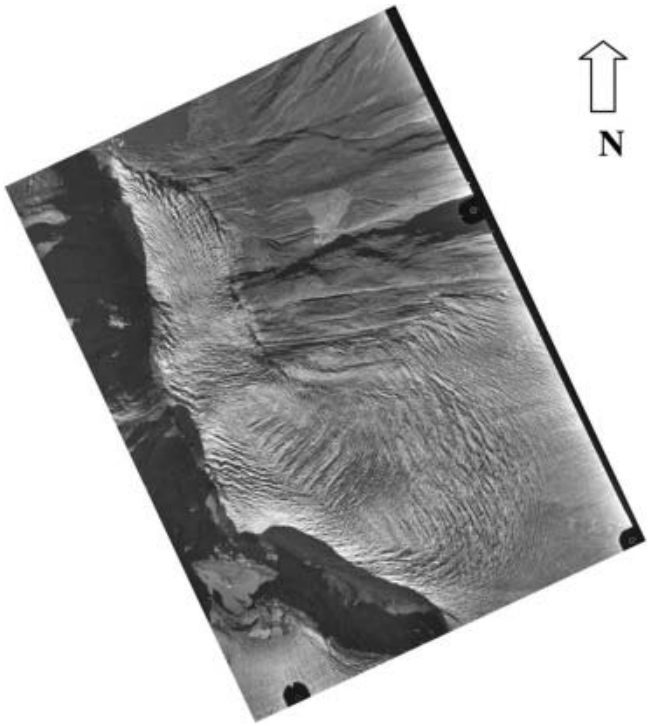


Fig. 2. Aerial photograph of the lowermost part of Engabreen taken on 20 August 2002. Glacier flow is approximately from bottom to top.

The area above this is flatter and thus has lower velocity, making it hard to measure displacement accurately over a 21 day period. If a longer period is used, features used for tracking change beyond recognition and so cannot be easily identified on subsequent photos.

Measurement technique for aerial photography

In order to derive glacier velocities from the multi-temporal aerial photography, we used the IMCORR software acquired from the US National Snow and Ice Data Center (NSIDC), Boulder, CO. IMCORR is an image correlation program that uses a normalized cross-covariance algorithm based on a fast Fourier transform (Bernstein, 1983; Scambos and others, 1992). The software aims to identify displacement as a function of systematic changes in image digital numbers (DNs). The algorithm normalizes a reference chip and larger search chip to a DN mean of zero and unity standard deviation prior to correlating the two chips. This normalization aims to minimize non-displacement variance in the chip DNs. The peak correlation between chips is then quantified using (Scambos and others, 1992):

$$\mathrm{CI}_{(\mathrm{L,S})} = \frac{\sum_{\mathrm{l,s}} (r_{(\mathrm{l}\pm,\mathrm{s})} - \mu_{(\mathrm{r})})(s_{(\mathrm{l,s})} - \mu_{\mathrm{s}})}{\left[\sum_{\mathrm{l,s}} (r_{(\mathrm{l,s})} - \mu_{(\mathrm{r})})^2\right]^{1/2} \left[\sum_{\mathrm{l,s}} (s_{(\mathrm{l,s})} - \mu_{(\mathrm{s})})^2\right]^{1/2}},$$

where $\mathrm{CI}_{(\mathrm{L,S})}$ is the correlation index at location L,S, $r_{(\mathrm{l,s})}$ is the DN for the reference chip at location l,s, μ_{r} is the average DN for the reference chip, $s_{(\mathrm{l,s})}$ is the DN for the search chip at location l,s, and $\mu_{(\mathrm{s})}$ is the average DN for the search chip. The output is a correlation map showing the similarity between the reference and search images. The correlation sub-routine forms part of the correlation strength parameter that can be used as part of a quality control procedure. The correlation strength (CS) is given by (T. Scambos and others, unpublished):

$$\mathrm{CS}_{(\mathrm{L,S})} = \sum \left(\frac{\mathrm{CI} - \bar{x}_{\mathrm{b}}}{\sigma_{\mathrm{b}}} + \frac{\mathrm{CI} - \alpha_{\max}}{\sigma_{\mathrm{b}}}\right) + 0.2(\eta_{\alpha} - 1),$$

where $\bar{x}_{\mathrm{b}}$ is the mean of the background DNs, σ_{b} is the standard deviation of the background values, $\alpha_{\max}$ is the maximum value >3 pixels from the peak and η_{α} is the number of 'large' values >3 pixels away. Such measures are used to manually identify and remove erroneous or low-confidence results from the final dataset (e.g. Scambos and others, 1992).

As input to IMCORR, we scanned subsets of the aerial photographs at 2500 dpi on an AGFA Horizon Plus scanner, resulting in a pixel resolution of 0.39 m. The aerial photographs were then manually co-registered to ±1 pixel using around 30 ground-control points and check points. The later image was warped to the earlier using a second-order polynomial warp with nearest-neighbour resampling. The first photograph was then registered to Universal Transverse Mercator (UTM) coordinates and warped (also using a polynomial warp with nearest-neighbour resampling). The co-registration error was estimated using both the displacement off-glacier measured by feature tracking and manual measurements of the displacement of identifiable features; the latter method is cruder and propagates an additional error. Off-glacier feature displacement varies across the scene with the degree of distortion in the original photographs, the distance from ground-control points and, where extreme, the surface slope. The highest co-registration errors occurred on the slopes east of Midnattsolsstinden to the south of the glacier snout. The largest error was 26 cm d^{-1}, although this error was exceptional; the error on this slope was typically 8–10 cm d^{-1}. Closer to the glacier, away from the steep slopes and image margins, this was reduced to <1 pixel over the 21 day period. The extreme error therefore occurs on a steep slope (~45°), with 200 m of relief amplitude, near the margins of the photographs. To the east of the glacier at higher relief, the co-registration error was 1–2 pixels, suggesting the image warping was accurate over the full range of altitudes in the images. On the glacier the relief amplitude is less pronounced and the co-registration more accurate.

The IMCORR algorithm was run on the co-located images using a search chip of 128 pixels, a reference chip of 64 pixels and a 50-pixel grid spacing. These values were selected after iterative trial runs with other configurations. A large search-chip size was required to eliminate the effects of shadow on the crevasses which constituted the majority of features tracked to produce the displacement map.

Initially the technique produced over 30 000 measurements. Deleting those points where the results flag showed that there was not a successful correlation gave 23 400 points. Deleting zero velocities brought the total down to 18 000 points. Further quality control of the data eliminated those points outside the boundary of the glacier, or where the direction of movement is physically unrealistic. The distribution of measurement points is shown in Figure 3. These adjustments show that although the initial process is automatic, attaining realistic velocities requires a large degree of post-processing that is done manually. It should be noted, however, that this is in part a function of the very

https://doi.org/10.3189/172756405781812655 Published online by Cambridge University Press

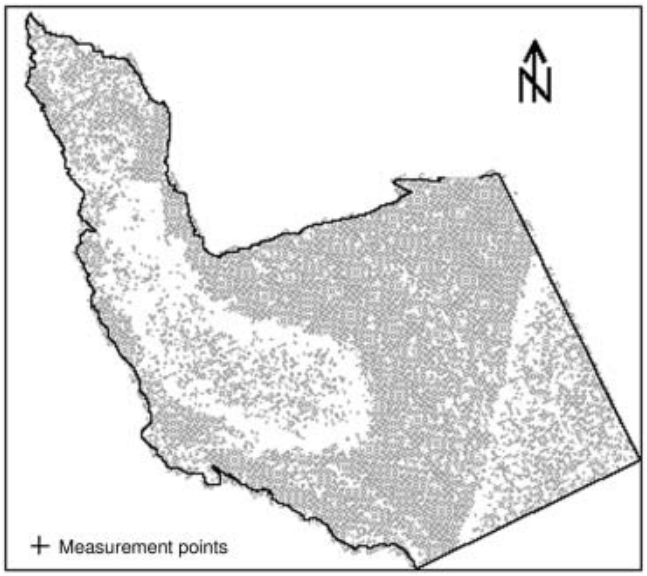


Fig. 3. Individual measurement points on the glacier.

Table 1. Annual horizontal velocity measured over periods greater than 1 year during 2000–03, and velocity at different periods shown as % of annual velocity. See Figure 4 for locations

Stake	Elevation	Annual velocity	Velocity as % of annual value		
			May–Aug.	Aug.–Sept.	Sept.–May
	m a.s.l.	m a^{-1}			
17	310	165	112	91	97
34	970	97		93	92
38	1050	58	106		95
11	1170	95		97	
21	1185	3			
16	1190	4	139		
90	1210	24		88	100
5	1237	48	103		96
40	1245	21	101		99
101	1316	23	131	109	96
105	1340	22	98	105	95
143	1395	11	124		

high resolution that we used in this investigation. At such high resolution the deformation of individual ice blocks (seracs) could be measured.

However, it is more reliable to filter or average the velocity measurements to normalize local effects and distortions. We did not use single values, but took the average of four or more values as part of the post-processing. The final, corrected, velocity measurements were estimated to be accurate to <8 pixels. Accuracies of ±1–4 pixels were achieved locally including over much of the lower tongue. The results from the IMCORR algorithm were checked for consistency and found to agree with manual measurements of displacement between the two photographs.

Stake measurements

Differential global positioning system (GPS) measurements were made of 13 stakes on the glacier that are used for mass-balance measurements, as well as four additional stakes set out purely for determination of velocity. The positions of the stakes were measured using an Ashtech GPS, with the same base station, Bautaen (see Fig. 1), for all measurements in order to minimize errors. GPS data were reduced using AOSS v.2 (Ashtech Office Suite for Survey), which is provided by Magellan products for use with Ashtech GPS receivers. The software was created by Spectra Precision Terrasat GmbH. Accuracy of horizontal position using differential GPS and using the same base station each time is about 10 cm. For measurements over a 1 month period (August–September), the total possible error is 20 cm, which gives an error in velocity of 0.67 cm d^{-1} over 30 days. As most measurement epochs were longer (May–August, May–September or September–May), errors were usually considerably less.

Measurements were performed several times a year, although it was not always possible to measure each stake at each visit. This could be due to the stake being still under snow when measurements were performed, or having melted out. When possible, a replacement stake was set out in the same location, and positional measurements were performed on it. If the original stake had been buried and was visible on the next visit, both stakes were then measured (and the replacement stake removed), thus giving movement over the whole period, as two separate measurements. Velocity measurements given here are for those stakes where measurements were made over several periods. Table 1 gives the annual velocity measured at several of the stakes. Results are also shown in Figure 4.

DISCUSSION

Velocity measurements

The contour map of horizontal velocity on the lowermost part of Engabreen is shown in Figure 5. Several interesting features can be noted. There is a slower-moving part of the glacier in the upper part of the glacier area photographed (righthand side of Fig. 5). Along the centre line, speeds decrease to about half their magnitude over a distance of about 200–400 m, before regaining their previous magnitudes over a similar distance. This coincides with a shallow part of the glacier: thicknesses decrease over a similar distance from >125 m of ice, to <75 m, then increase again to >120 m (see Fig. 6). To the north of this area, velocities are <20 cm d^{-1}, and in some parts <10 cm d^{-1}. This area coincides with a shallow part of the glacier where ice thickness is only 25 m (near F′ in Fig. 5).

The highest velocities are slightly displaced from the centre line to the southeast. This coincides with an asymmetrical deepening of the bedrock on this side, and is also due to the curvature of the glacier.

The highest velocities are not concentrated in the centre, as expected, but show an approximately elliptical pattern of velocity highs of up to 40 cm d^{-1}, with velocities in the centre of this ellipse <20 cm d^{-1}. This pattern corresponds fairly well with the pattern of points used to measure the velocity (Fig. 3). However, this is not an artefact of the measurement technique or the contouring. Several features on the glacier were measured manually on both photographs and confirmed this pattern of two maxima and a lower value in the centre. The contour map shows total horizontal displacement, rather than only displacement

https://doi.org/10.3189/172756405781812655 Published online by Cambridge University Press

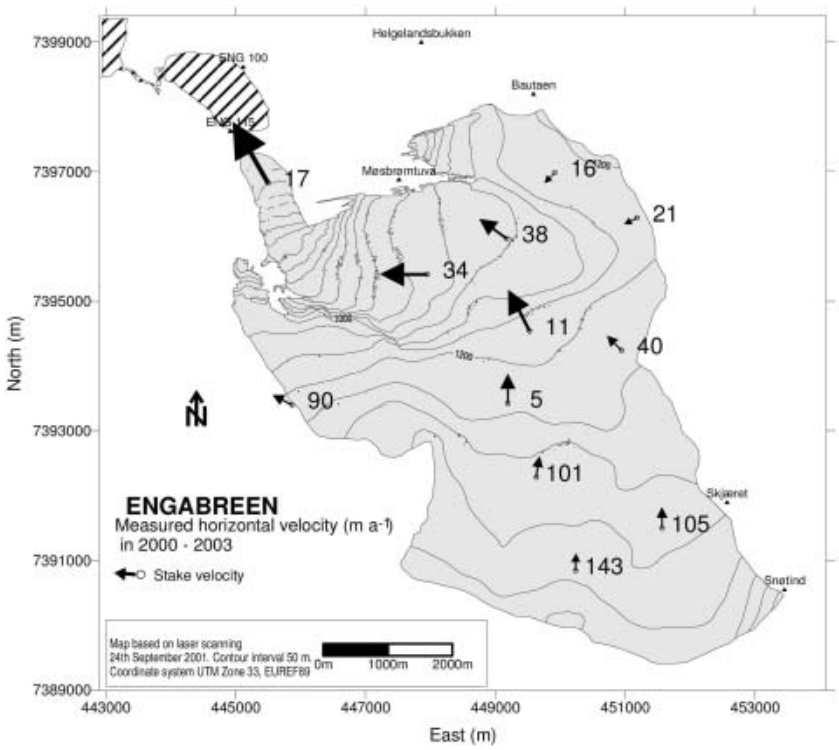


Fig. 4. Examples of stake velocities. Numbers indicate stake positions for use with Table 1, and length of arrow indicates velocity.

parallel to the centre line. The glacier is convex, with steep edges, so total velocity at the sides will be high, whereas the surface slope is low in the centre.

Several horizontal velocity profiles across the glacier are plotted (see Fig. 5 for locations). These are shown in Figure 7. All six profiles show a displacement of the velocity maximum to the outside of the curve of the glacier, as also seen by Echelmeyer and Kamb (1987) on Blue Glacier, Washington, USA, and as confirmed theoretically by them. The pattern in this case is somewhat complicated by the double maxima in velocity. However, Echelmeyer and Kamb found the maximum gradient in the flowline velocity across the glacier to be towards the inside of the curve, whereas on Engabreen it appears to be the opposite. This may be because total velocity rather than flowline velocity is plotted here. Also, the bedrock topography is distinctive here and may cause some of the anomalous behaviour.

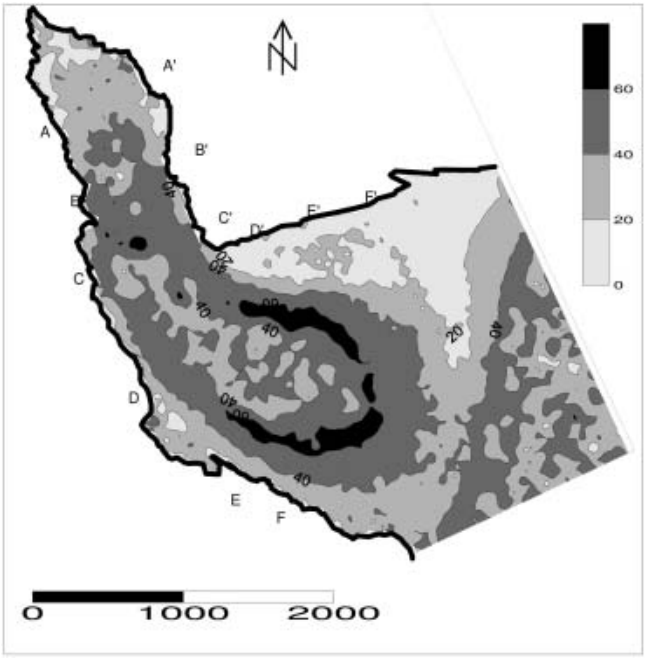


Fig. 5. Contour map of velocity on the lowermost part of Engabreen. Velocity contours are shown in cm d^{-1}. Letters at the side of the glacier mark profiles shown in Figure 7.

The two different techniques used, velocities measured from aerial photography and from position measurements of stakes, generally do not cover the same part of the glacier. However, there is a stake at 310 m a.s.l. (stake 17 in Fig. 4) that is also covered by the aerial photography. This stake has an annual velocity of 165 m a^{-1}, which is equivalent to 45 cm d^{-1}. The velocity of this stake over the period August–September is 91% of the annual velocity, or 41 cm d^{-1}. This agrees well with the velocity measured from aerial photography, 40 cm d^{-1}.

Seasonal velocity variations

The velocity measurements as measured at stakes distributed over the glacier show seasonal variations, as expected, with measured surface velocities being higher in the summer (May–September) than in the winter months (September–May). Velocity is generally highest in the spring/early summer (e.g. Hooke and others, 1989; Copland and others, 2003) due to increased glacier sliding due to meltwater, and because the snowpack also slightly increases the total thickness of the glacier, and hence the velocity. The velocity measurements were performed at the same time as the mass-balance measurements: generally at the end of May, in August, and in mid- to late September. It is possible that the spring speed-up of the glacier occurred slightly before the measurements in May, so that the

https://doi.org/10.3189/172756405781812655 Published online by Cambridge University Press

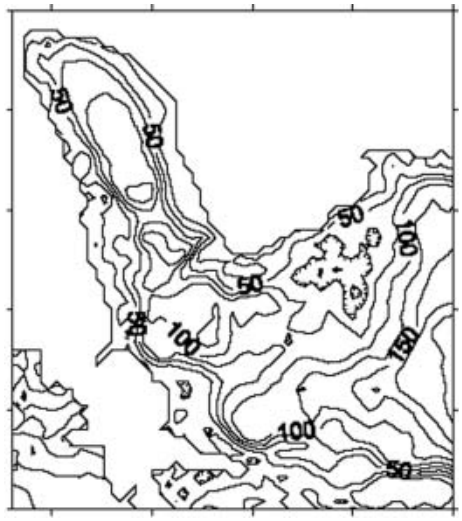


Fig. 6. Glacier thickness in metres.

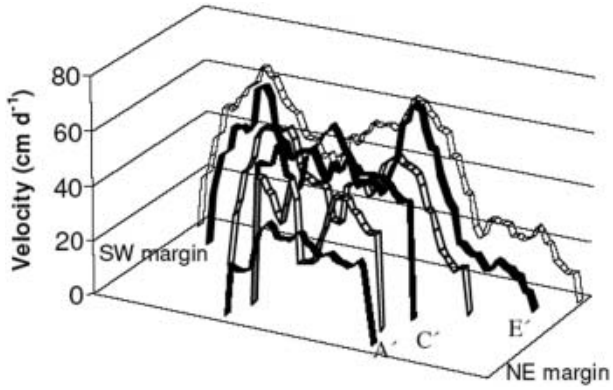


Fig. 7. Velocity profiles across the glacier from repeat photogrammetry measurements.

'winter' measurements may reflect some of the speed-up of the glacier.

Table 1 shows the annual velocity for several stakes and the velocity over different periods of the year as a percentage of the annual value. Velocities were generally higher during the summer than the winter. This agrees with the spring speed-up of the glacier increasing average values over this period. Where velocity values between May and August are available, all except one show values greater than 100% of the annual velocity. Velocities were generally lower than the annual average in the August–September period, when there is less meltwater. For the stakes at higher elevations, above 1300 m a.s.l., velocity was higher than the annual average in the August–September period. This may reflect the speed-up of the glacier occurring later in the year at higher elevations. All stakes showed lower velocities over the winter period compared with the annual average.

Comparison with previous velocity measurements on Engabreen

Kohler (1998) discusses previous velocity measurements on the lower part of Engabreen from repeat aerial photography. Photography was performed over one epoch in 1990 and 1991, and over two epochs in each of the following 4 years. The photography was performed on different dates each year, but always between 20 June and 15 August. Measured values were approximately the same as those shown here. However, the areas covered were much smaller, and do not show the whole width of the glacier at any point. Hence, the features that are discussed here were not observed.

A. Sharov (unpublished map) has estimated the velocity of a number of outlet glaciers from the Svartisen ice caps. Results from Fingerbreen, one of the Svartisen glaciers, are also reported by Sharov (2003) who applied a gradient approach to radar interferometry (GINSAR). The new approach aims to resolve the difficulties commonly faced in conventional interferometry. The unpublished data show velocities exceeding 40 cm d^{-1} in the upper part of the glacier tongue (righthand side of Fig. 5). The average velocity of the upper glacier appears be 20–40 cm d^{-1}, with a steep gradient at the margins and two bull's-eyes where velocities exceed 40 cm d^{-1}. These features are normally associated with the vertical expression of mass-balance pulses, and therefore suggest that the GINSAR is combined vertical and horizontal displacement whilst the aerial photographs display only horizontal displacement.

No velocity data on the glacier tongue of Engabreen are available in Sharov's work. Those data higher up on the glacier broadly agree with our data derived from multi-temporal aerial photography, although the overlap is small. It should be noted, however, that our data are integrated over 20 days whilst those of Sharov (unpublished map) are integrated over three European Remote-sensing Satellite-1 and -2 (ERS-1 and ERS-2) tandem image pairs acquired between 16 March and 2 April 1996. The precise composition of Sharov's dataset is unclear, but we assume that these measurements are a mean of three 24 hour measurements over the 17 day period. Thus, divergence between the aerial photography method and Sharov's GINSAR may be a function of the difference in season or measurement period. Higher velocities would be expected in our data due to enhanced sliding resulting from increased meltwater availability at the bed in the summer. Furthermore, the aerial photographs had a 20 day separation, whereas the GINSAR methods resulted from three diurnal measurements separated by 17 days, introducing the probability of divergence due to temporal resolution.

CONCLUSIONS

The image correlation program IMCORR was successfully applied to aerial photographs. The results can be used to demonstrate the main features of the velocity pattern on the lowermost part of Engabreen. Using the technique, we were able to measure a large number of horizontal displacements automatically, but a certain amount of manual post-processing was required to discard values that were physically non-realistic, or not on the glacier. These velocity measurements were complemented by differential GPS measurements of the positions of mass-balance stakes on the upper part of the glacier where the IMCORR technique is not appropriate due to the lack of suitable features to track and the lower velocities.

ACKNOWLEDGEMENTS

The data used in this study were collected as part of the OMEGA project, which is funded by the Fifth Framework Programme of the European Commission, contract

https://doi.org/10.3189/172756405781812655 Published online by Cambridge University Press

No. EVK2-CT-2000-00069. Measurement of the glacier velocities from aerial photography was performed as part of Northern View, a European Space Agency (ESA) Global Monitoring for Environment and Security (GMES) funded programme. IMCORR software was downloaded from the NISDC. M. Kennett performed the radar measurements used to calculate ice thickness. We thank B. Raup for help with the software. B. Kjøllmoen performed the GPS calculations, D. Ejigu tabulated the stake positions and displacements, and several other people from NVE participated in the fieldwork.

REFERENCES

Bernstein, R. 1983. Image geometry and rectification. *In* Colwell, R.N., *ed. Manual of remote sensing*. Falls Church, VA, American Society of Photogrammetry, 873–922.

Brecher, H.H. 1986. Surface velocity determination on large polar glaciers by aerial photogrammetry. *Ann. Glaciol.,* **8**, 22–26.

Copland, L., M.J. Sharp and P.W. Nienow. 2003. Links between short-term velocity variations and the subglacial hydrology of a predominantly cold polythermal glacier. *J. Glaciol.,* **49**(166), 337–348.

Echelmeyer, K. and B. Kamb. 1987. Glacier flow in a curving channel. *J. Glaciol.,* **33**(115), 281–292.

Hooke, R.LeB., P. Calla, P. Holmlund, M. Nilsson and A. Stroeven. 1989. A 3 year record of seasonal variations in surface velocity, Storglaciären, Sweden. *J. Glaciol.,* **35**(120), 235–247.

Kjøllmoen, B., L.M. Andreassen, R.V. Engeset, H. Elvehøy and M. Jackson. 2003. Glaciological investigations in Norway in 2002. *NVE Rapp.* 3-2003.

Kohler, J. 1998. The effect of subglacial intakes on ice dynamics at Engabreen. *NVE Rapp.* 12-1998.

Krimmel, R.M. 2001. Photogrammetric data set, 1957–2000, and bathymetric measurements for Columbia Glacier, Alaska. *US Geol. Surv. Water-Resour. Invest. Rep.* 01-4089.

Lucchitta, B.K. and C.E. Rosanova. 1998. Retreat of northern margins of George VI and Wilkins Ice Shelves, Antarctic Peninsula. *Ann. Glaciol.,* **27**, 41–46.

Scambos, T.A. and R. Bindschadler. 1993. Complex ice stream flow revealed by sequential satellite imagery. *Ann. Glaciol.,* **17**, 177–182.

Scambos, T.A., M.J. Dutkiewicz, J.C. Wilson and R.A. Bindschadler. 1992. Application of image cross-correlation to the measurement of glacier velocity using satellite image data. *Remote Sens. Environ.,* **42**(3), 177–186.

Sharov, A.I. 2003. Gradient approach to INSAR modelling of glacial dynamics and morphology. *In Geoinformation for European-Wide Integration, Proceedings of the 22nd Symposium of the European Association of Remote Sensing Laboratories, Prague, Czech Republic, 4–6 June 2002*. Rotterdam, Millpress, 373–381.

https://doi.org/10.3189/172756405781812655 Published online by Cambridge University Press